



## Langmuir–Blodgett films of C<sub>60</sub> and C<sub>60</sub>O on Silicon: Islands, rings and grains

Cong Yan<sup>a</sup>, Aneta Dybek<sup>b</sup>, Claire Hanson<sup>c</sup>, Karina Schulte<sup>a</sup>, A.A. Cafolla<sup>c</sup>, John Dennis<sup>b</sup>, Philip Moriarty<sup>a,\*</sup>

<sup>a</sup> The School of Physics and Astronomy, The University of Nottingham, Nottingham NG7 2RD, UK

<sup>b</sup> Department of Physics, Queen Mary, University of London, Mile End Road, London E1 4NS, UK

<sup>c</sup> The School of Physical Sciences, Dublin City University, Glasnevin, Dublin 9, Ireland

### ARTICLE INFO

#### Article history:

Received 30 June 2008

Received in revised form 30 September 2008

Accepted 6 October 2008

Available online 17 October 2008

#### Keywords:

Langmuir–Blodgett

Fullerenes

Silicon

Monolayer

Atomic force microscopy

### ABSTRACT

We show that monolayer-high islands of C<sub>60</sub> and C<sub>60</sub>O can be transferred from Langmuir films on a water or phenol sub-phase to oxide-terminated Si(111) substrates. Faceted islands, in some cases incorporating a foam-like morphology reminiscent of that previously observed for Langmuir films at the water–air interface using Brewster angle microscopy, are formed and transferred using small amounts (100–400 μl) of low concentration (of order 10<sup>−5</sup>M) solutions of C<sub>60</sub> (or C<sub>60</sub>O) with low target pressures (~10 mN/m). However, worm-like monolayer domains are also observed under identical experimental conditions, indicating the key role that inhomogeneous solvent evaporation plays in the formation of two-dimensional fullerene aggregates on the subphase surface. While Langmuir–Blodgett multilayers of C<sub>60</sub> and C<sub>60</sub>O are both granular, there are significant morphological differences observed between the molecular thin films. In particular, C<sub>60</sub>O multilayers contain a relatively high density of ring (or “doughnut”) features with diameters in the 100–300 nm range which are not observed for C<sub>60</sub>. We attribute the origin of these features to dipolar or hydrogen bonding-mediated interactions between the C<sub>60</sub>O molecules at the water surface.

© 2008 Elsevier B.V. All rights reserved.

### 1. Introduction

The study and control of fullerene–surface interactions remains a cornerstone of nanoscience due to the fascinating and, in many cases, exotic physicochemical behaviour of the family of buckminsterfullerene molecules. A substantial body of work has focused on the structure, chemistry, electronic properties, and/or optical response of (sub)monolayers of C<sub>60</sub> and associated derivatives deposited onto solid substrates via vapor phase methods (see [1–3] for overviews). In many cases, however, deposition from the liquid/solution phase is necessary. This is particularly true for fullerenes which cannot be sublimed, such as N@C<sub>60</sub> [4] and C<sub>60</sub>O [5–7]. Hence, a considerable number of groups have explored the possibility of using the Langmuir–Blodgett (LB) technique to transfer fullerene monolayers/films from an air–water (or air–phenol) interface to a variety of substrates including mica [9–10], silicon [5,11], and graphite [12].

C<sub>60</sub>'s lack of amphiphilic character makes the preparation of high quality LB monolayers and films problematic at best. The hydrophobicity of unfunctionalised C<sub>60</sub> can lead to extensive aggregation and multilayer formation on the polar subphases [13–17,12] and a number of strategies have been adopted, including the use of amphiphilic derivatives [18–22] and the incorporation of fullerene molecules in amphiphilic matrices [23–25,11], to inhibit aggregation into 3D clusters. Moreover, there have been a number of important

investigations focussed on how the balance between hydrophobicity and hydrophilicity affects the assembly of fullerene derivatives [26]. Nevertheless, and despite the difficulties arising from strong inter-fullerene interactions, there have been a small number of important examples of the transfer of unfunctionalised (and pure) monolayer fullerene films to solid substrates. Uemura et al. [27] prepared epitaxial adlayers of C<sub>60</sub>, effectively identical to those formed via sublimation, on Au(111) via the transfer of Langmuir films at the air–water interface. A “multi-step creep method” has also been used to form monolayer islands and complete monolayers of C<sub>60</sub> on mica surfaces by transferring Langmuir films on water [9,8]. To date, however, convincing evidence for the presence of monolayer Langmuir–Blodgett films (or islands) on silicon and silicon dioxide surfaces is lacking. Given the importance of silicon dioxide as a dielectric layer in molecular electronics devices, we have revisited the issue of transfer of fullerene Langmuir films to hydrophilic silicon surfaces.

We describe the transfer of monolayer islands of C<sub>60</sub> and C<sub>60</sub>O to silicon substrates using small amounts of relatively low concentration (~10<sup>−5</sup>M) spreading solutions on a water or phenol subphase. Atomic force microscopy (AFM) images show that a foam-like morphology, reminiscent of that observed previously in Brewster angle microscopy (BAM) studies of fullerene Langmuir films [16,18], can be retained on transfer of fullerene islands to a solid substrate. A variety of non-equilibrium monolayer island shapes are also observed, highlighting the role that rapid (and inhomogeneous) solvent evaporation plays in determining the structure of 2D Langmuir films of fullerenes. There are striking morphological differences between multilayer LB films of

\* Corresponding author.

E-mail address: [philip.moriarty@nottingham.ac.uk](mailto:philip.moriarty@nottingham.ac.uk) (P. Moriarty).

URL: <http://www.nottingham.ac.uk/physics/research/nano> (P. Moriarty).

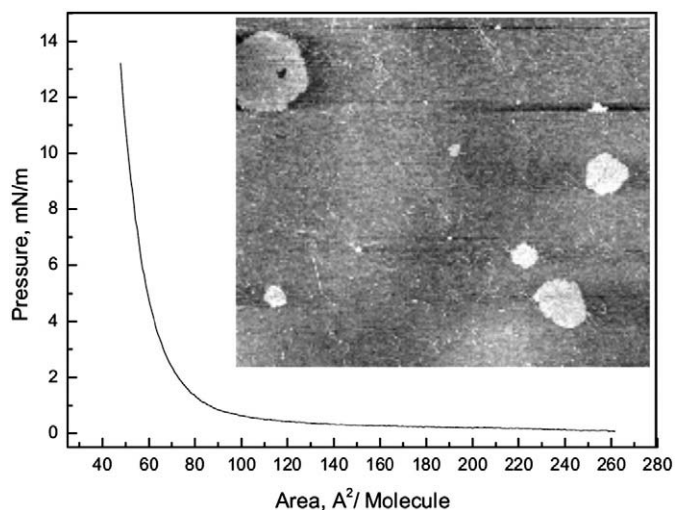


**Fig. 1.**  $\pi$ - $A$  Isotherm for a 350  $\mu\text{l}$  volume of a  $5 \times 10^{-5}\text{M}$  solution of  $\text{C}_{60}$  in benzene on a water subphase. Inset: Tapping mode AFM image ( $13 \times 16 \mu\text{m}^2$ ) of monolayer (1 nm) high  $\text{C}_{60}$  islands on an oxide-terminated Si(111) surface transferred at a pressure of 10 mN/m. Note both the faceting and the very low areal density of the islands.

$\text{C}_{60}$  and  $\text{C}_{60}\text{O}$  with the latter containing many “doughnut”-shaped molecular aggregates. We attribute their presence to the rather more polar character of the fullerene epoxide due to the oxygen substituent and the associated molecular dipole moment ( $1.26 \pm 0.14 \text{ D}$  [7]).

## 2. Experimental section

All of our Langmuir film studies were carried out using the NIMA 312D trough. Hydrophilic Si(111) surfaces were prepared by first cleaning the substrates in organic solvents in an ultrasonic bath and in an ozone plasma for 10 min, and then subjecting them to a standard  $\text{H}_2\text{SO}_4:\text{H}_2\text{O}_2$  (“piranha”) treatment [33].  $\text{C}_{60}$  (purity 99.9%) was purchased from MER Corporation (Tucson, AZ).  $\text{C}_{60}\text{O}$  was produced by the contact arc method and then separated and purified by high purity liquid chromatography (HPLC) to better than 99% purity.  $\text{C}_{60}$  was dissolved in benzene, while  $\text{C}_{60}\text{O}$  was dissolved in toluene. All solvents used were HPLC grade. As a low concentration of the spreading solution is essential to obtain monolayer or submonolayer Langmuir films [13,15,5], a spreading solution with a concentration of between  $3 \times 10^{-5} \text{ M}$  and  $6 \times 10^{-5} \text{ M}$  was used for both  $\text{C}_{60}$  and  $\text{C}_{60}\text{O}$ . High purity water or HPLC grade phenol was used as the subphase.

Before spreading, the subphase surface was swept and cleaned. Then a total of 100  $\mu\text{l}$  to 400  $\mu\text{l}$  of solution was introduced. The volume of each droplet added to the air–water interface was controlled within 5  $\mu\text{l}$ , and each droplet was introduced at different well-separated spots on the interface. 20 to 30 min were left for the solvent to evaporate completely. Single or multiple compressions were then carried out at a compression rate of  $166 \text{ mm}^2 \text{ s}^{-1}$  to form the Langmuir film, followed with film transfer to Si(111) substrates by vertical dipping at a speed of 5 mm/min. Tapping mode atomic force microscopy AFM (TM-AFM) was carried out using an Asylum Research MFP-3D system with Olympus AC240 silicon probes (spring constant: 2 N/m; resonant frequency: 70 kHz).

## 3. Results and discussion

In Fig. 1 we show the  $\pi$ - $A$  isotherm for a  $\text{C}_{60}$  submonolayer transferred from a Langmuir film on water. Close packing of the adsorbed fullerene molecules is evident from the faceting of the islands shown in the AFM image included as an inset to the isotherm. Each island is 1 nm high, consistent with the hard sphere diameter of the  $\text{C}_{60}$  molecule. What is arguably less consistent with the molecular

diameter, however, is the area per molecule evaluated by extrapolation of the isotherm to the  $x$ -axis. The area per molecule is less than the limiting value for a close-packed monolayer (ML), i.e.  $86.6 \text{ \AA}^2$ . This is a surprising result given that the AFM data suggest that the total coverage is much less than 1 ML. One might expect that, as observed by Yanagida et al. [8], the area per molecule would be significantly greater than  $86.6 \text{ \AA}^2$ .

A similar apparent discrepancy between the AFM and isotherm data was found for submonolayer coverages of  $\text{C}_{60}$  transferred from a phenol subphase (compare Fig. 2(a) and (b)). One possibility we initially considered was that the  $\text{C}_{60}$  islands seen in the AFM images of Figs. 1 and 2 are adsorbed not on the native oxide-terminated Si(111) substrate but on a complete  $\text{C}_{60}$  monolayer. Phase images (see Fig. 2(d)) are, however, not consistent with this suggestion, and show that there is a significant difference in energy dissipation on the islands as compared to the island-free regions of the sample. Although the interpretation of tapping mode phase maps is far from straightforward and must be treated with some caution, such a dramatic variation in phase signal would be rather surprising if the entire surface were covered with  $\text{C}_{60}$ . Moreover, we found that *under nominally identical conditions* (i.e. same solution concentration, deposited volume, target pressure, and compression speed) while monolayer islands such as those shown in Figs. 1 and 2 can sometimes be formed, in other cases grainy multilayer films (similar to that shown in Fig. 5(a)) are produced.

This lack of reproducibility is somewhat perplexing but can be rationalised in terms of the highly non-uniform nature of Langmuir films of  $\text{C}_{60}$  as revealed by the BAM measurements of Castillo et al. [16]. The apparent discrepancy between the low area-per-molecule values derived from the isotherms and the low surface coverage observed in the AFM measurements (Figs. 1 and 2) is likely due to the difference in morphology at the edges and centre of the trough: while monolayer islands can “survive” at the centre of the trough (where transfer to the sample surface takes place), compression leads to multilayer formation along the trough edges. (The Wilhelmy plate used for pressure sensing is located approximately 3 cm from the sample position, towards the edge of the trough). In addition, the model put forward by Evans [17] to describe the formation of

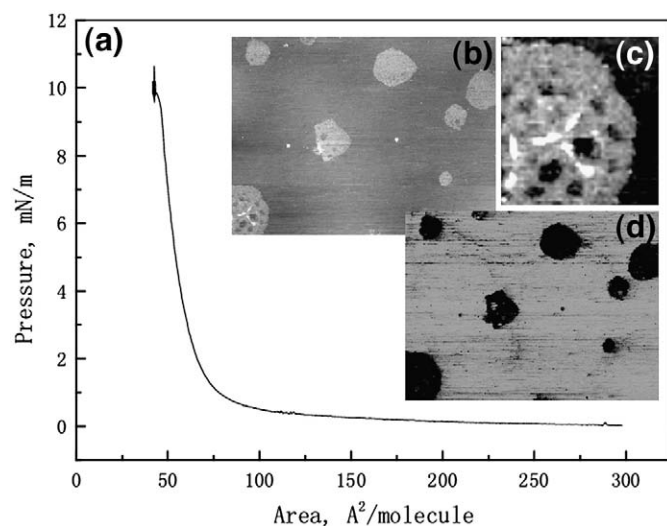


**Fig. 2.** (a)  $\pi$ - $A$  isotherm for 250  $\mu\text{l}$  of a  $5 \times 10^{-5}\text{M}$  solution of  $\text{C}_{60}$  in benzene on a phenol subphase. (b) AFM image ( $15 \times 20 \mu\text{m}^2$ ) of monolayer high  $\text{C}_{60}$  islands transferred to an oxide-terminated Si(111) surface. (c)  $4 \times 4 \mu\text{m}^2$  zoom of island shown in bottom left hand corner of the image shown in (b). The island contains a number of large holes and has a sponge- or foam-like character reminiscent of the foams observed by Castillo et al. [16] using Brewster angle microscopy. Note the presence of multilayer  $\text{C}_{60}$  aggregates on top of the island (the brightest regions in the image). (d) Phase image corresponding to the topography shown in (a).

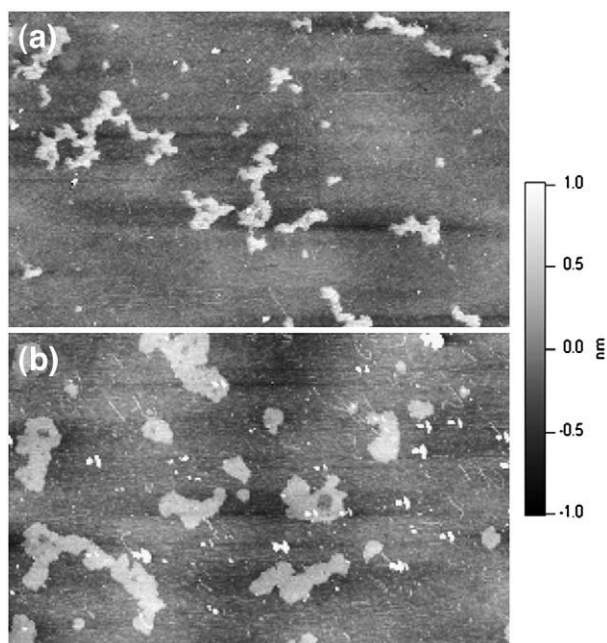


**Fig. 3.** AFM images of non-equilibrium 2D islands of  $C_{60}$  transferred from Langmuir films on water (see caption to Fig. 1 for details of solution concentration and volume). Images (a) and (b) are  $14 \times 20$  and  $12 \times 20 \mu\text{m}^2$  respectively. The average coordination of  $C_{60}$  molecules is significantly greater for image (b). (Note also that although a “double tip” artefact is present in (b), it does not strongly affect the imaging of the (low aspect ratio) 2D  $C_{60}$  islands.)

Langmuir films of  $C_{60}$  indicates that while the kinetics are such that solvent evaporation and fullerene aggregation should predominantly produce a molecular monolayer, this is not the equilibrium state of the system and small perturbations – for example, capillary waves on the sub-phase due to vibrations – can lead to the formation of multilayers.

Although Yanagida et al. [9,8] have also succeeded in transferring submonolayer coverages of  $C_{60}$  to solid substrates from Langmuir films, in their case they observed circular, rather than faceted (Fig. 1), islands. Castillo et al. [16] observe a variety of condensed phase structures in  $C_{60}$  Langmuir films including foams, discs, and stripes. Each of these structures is a highly non-equilibrium arrangement of  $C_{60}$  molecules. (The equilibrium 2D structure on a solid surface would be a very large faceted island of close-packed molecules). We postulate that both the foam-like structure observed by Castillo et al. [16] and the hole-ridden island shown in Fig. 2(c) arise from the dewetting dynamics of the volatile solvent. Similar foam (or cellular network) morphologies to those seen by Castillo et al. (albeit on smaller length-scales) have been observed for colloidal nanoparticle assemblies formed via deposition from volatile solvents such as toluene or hexane [28,29]. The presence of foam-like and non-equilibrium assemblies in fullerene Langmuir films may be explained as follows. Holes open in the solvent due either to thermal nucleation or a spinodal dewetting mechanism [30,29,31], the retracting solvent front carries fullerene molecules with it, and the final spatial distribution of  $C_{60}$  is a signature of the distribution of the solvent in the late stages of drying.

As shown in Fig. 3, we have successfully transferred a variety of non-equilibrium structures from Langmuir films of  $C_{60}$  on water to oxide-terminated silicon. These structures arise because inhomogeneous spreading will lead to thickness variations in the solvent film, producing a range of local evaporation times. Longer evaporation times will lead to the system approaching equilibrium and forming large faceted islands, as shown in Figs. 1 and 2. Shorter evaporation times result in significant kinetic hindrance, trapping the fullerene molecules in metastable structures. The diffusion barrier of  $C_{60}$  on

oxide-terminated Si(111) is apparently large enough so that the non-equilibrium fullerene structures, when transferred to the solid substrate (Fig. 3), cannot ripen towards a lower energy state [32].

It was also possible to form monolayer-high islands of  $C_{60}O$  on hydrophilic oxide-terminated silicon substrates, see Fig. 4. The total deposited volume ( $300 \mu\text{l}$ ), solution concentration ( $3 \times 10^{-5} \text{ M}$  in toluene), target pressure ( $10 \text{ mN/m}$ ), and speed of compression were all very similar (or identical) to those used to transfer  $C_{60}$  monolayer islands to Si(111). The discrepancy between the area-per-molecule value and the AFM images discussed above for  $C_{60}$  is also observed for the  $C_{60}O$  data. A key difference between  $C_{60}$  and  $C_{60}O$  monolayer islands is, however, highlighted in the inset to Fig. 4(b). Although the island height is again  $1 \text{ nm}$ , the surface is considerably rougher because the monolayer aggregate comprises a disordered collection of small 2D clusters of molecules. Moreover, we observe a greater number of 3D clusters on  $C_{60}O$  monolayer samples than for the corresponding 2D  $C_{60}$  islands.

Single compressions at higher target pressures ( $25 \text{ mN/m}$ , Fig. 4(c)), lead to the formation of a granular film with an average thickness of  $3.7 \pm 0.4 \text{ nm}$ . The average thickness value, however, is somewhat misleading in that the film is covered with a high density of much thicker ( $\sim 12\text{--}15 \text{ nm}$ )  $C_{60}O$  clusters. Similar behaviour was observed

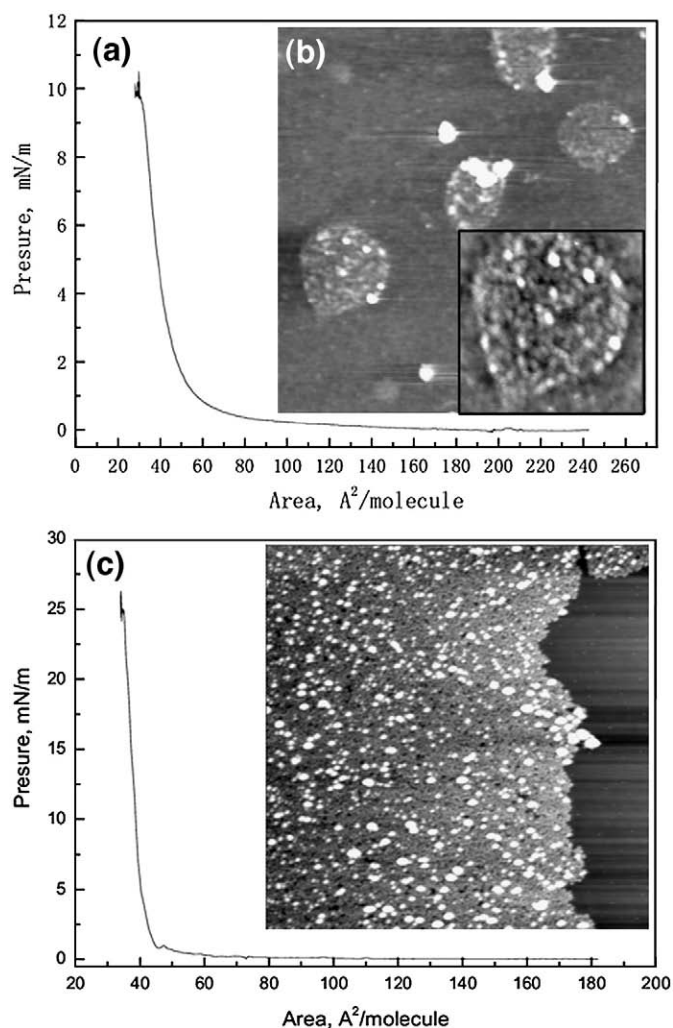


**Fig. 4.** (a)  $\pi$ - $A$  isotherm for a Langmuir  $C_{60}O$  film on water. The total deposited volume was  $300 \mu\text{l}$ , the concentration was  $3 \times 10^{-5} \text{ M}$  (in toluene), and the target pressure was  $10 \text{ mN/m}$ ; (b) AFM image ( $3.5 \times 3.5 \mu\text{m}^2$ ) of monolayer  $C_{60}O$  islands on oxide-terminated Si(111). Inset: Higher resolution ( $1 \mu\text{m}^2$ ) image of a  $C_{60}O$  monolayer island; (c) Isotherm for  $C_{60}O$  Langmuir film compressed to a higher ( $25 \text{ mN/m}$ ) target pressure; Inset: Corresponding AFM image ( $10 \times 10 \mu\text{m}^2$ ).

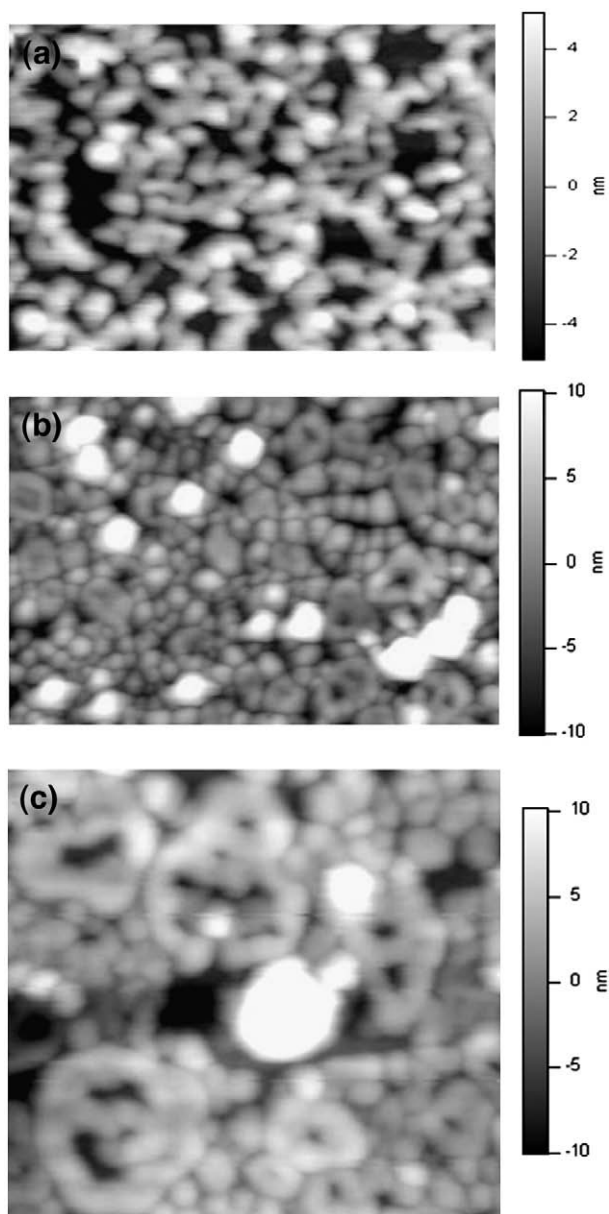


**Fig. 5.** (a) AFM image ( $0.8 \times 1.2 \mu\text{m}^2$ ) of a  $\text{C}_{60}$  multilayer Langmuir film transferred at a target pressure of 10 mN/m to an oxide-terminated Si(111) surface. The concentration and volume of the  $\text{C}_{60}$  in benzene solution were  $5 \times 10^{-5}$  M and  $300 \mu\text{l}$  respectively.; (b) AFM image ( $1.0 \times 1.5 \mu\text{m}^2$ ) of  $\text{C}_{60}\text{O}$  multilayer on oxide-terminated Si(111) ( $4 \times 10^{-5}$  M solution of  $\text{C}_{60}\text{O}$  in toluene; total volume:  $400 \mu\text{l}$ ; target pressure: 10 mN/m). (c) Higher resolution ( $1.3 \times 1.4 \mu\text{m}^2$ ) image of “doughnut”-shaped  $\text{C}_{60}\text{O}$  aggregates.

for  $\text{C}_{60}$  films produced at 25 mN/m and is consistent with the enhanced aggregation observed in previous studies of Langmuir films of fullerenes produced at high target pressures. Higher resolution AFM images of Langmuir–Blodgett multilayers, however, show a significant difference between the morphology of  $\text{C}_{60}$  and  $\text{C}_{60}\text{O}$  films. As is clear from a comparison of Fig. 5(a) and (b), 3D aggregates of  $\text{C}_{60}\text{O}$  exhibit a “doughnut”-shaped morphology that is not observed for multilayer films of  $\text{C}_{60}$  prepared at the same target pressure. (Langmuir–Blodgett multilayers of  $(\text{C}_{59}\text{N})_2$  (data not shown) also did not form “doughnut”-shaped aggregates). Fig. 5(c) is a higher resolution image of a  $\text{C}_{60}\text{O}$  multilayer showing that a range of ring sizes are present.

Although we do not have a good understanding of the mechanism underpinning the formation of the “doughnut”-shaped  $\text{C}_{60}\text{O}$  aggregates, it would be surprising if the dipole moment of the  $\text{C}_{60}\text{O}$

molecule, estimated as  $1.26 \pm 0.14$  D for the  $\text{C}_{60}\text{O}$ -5,6 isomer ( $C_s$  symmetry) or  $0.79 \pm 0.13$  D for the  $\text{C}_{60}\text{O}$ -6,6 isomer ( $C_{2v}$  symmetry) [7], did not play a role. “Chaining” of  $\text{C}_{60}\text{O}$  molecules, a precursor to ring formation, could plausibly arise from direct dipolar interactions or, as previously suggested by Maliszewskij et al. [5], may be mediated via hydrogen bonds to water. A BAM study, similar to that performed by Castillo et al. [16] for  $\text{C}_{60}$  Langmuir films, would be particularly useful in elucidating differences in the interaction of  $\text{C}_{60}$  and  $\text{C}_{60}\text{O}$  with the water subphase.

#### 4. Conclusion

We have successfully transferred monolayer islands of  $\text{C}_{60}$  and  $\text{C}_{60}\text{O}$  to hydrophilic ( $\text{SiO}_2$ -terminated) silicon substrates from Langmuir films on water and phenol. In addition to micron-scale faceted islands, a variety of far-from-equilibrium 2D aggregates form on the water (or phenol) surface and are transferred to the silicon substrate. We postulate that variations in solvent wetting behaviour (and thus film thickness) across the water subphase lead to different evaporation times and, thus, a variety of fullerene 2D island shapes. There are striking morphological differences between multilayer Langmuir–Blodgett films of  $\text{C}_{60}$  and  $\text{C}_{60}\text{O}$  with the polar character of the latter leading to the formation of “doughnut”-shaped aggregates with diameters in the 100–300 nm range.

#### Acknowledgements

We acknowledge funding from the European Union's Framework 6 Programme: Marie Curie Early Stage Training, contract MRTN-CT-2004-506854 (NANOCAGE). KS thanks the University of Nottingham for the award of an Anne McLaren fellowship. AAC acknowledges funding from the Higher Education Authority's Programme for Research in Third-level Institutions (Cycle II). We also gratefully acknowledge N. Tagmatarchis, Theoretical and Physical Chemistry Institute, National Hellenic Research Foundation, Greece for the supply of  $(\text{C}_{59}\text{N})_2$ .

#### References

- [1] E.I. Altman, R.J. Colton, *Surf. Sci.* 295 (1993) 13.
- [2] Q.K. Xue, T. Hashizume, T. Sakurai, *Prog. Surf. Sci.* 56 (1997) 1.
- [3] H. Rafii-Tabar, K. Ghafouri-Tabrizi, *Prog. Surf. Sci.* 67 (2001) 217.
- [4] T.A. Murphy, T. Pawlik, A. Weidinger, M. Hohne, R. Alcalá, J.M. Spaeth, *Phys. Rev. Lett.* 77 (1996) 1075.
- [5] N.C. Maliszewskij, P.A. Heiney, D.R. Jones, R.M. Strongin, M.A. Cichy, A.B. Smith, *Langmuir* 9 (1993) 1439.
- [6] K.M. Creggan, J.L. Robbins, J.M. Millar, R.D. Sherwood, P.J. Tindall, A.B. Smith, J.P. McCauley, D.R. Jones, R.T. Gallagher, D.M. Cox, *J. Am. Chem. Soc.* 114 (1992) 1103.
- [7] B.-C. Wang, L. Chen, K.-J. Lee, C.-Y. Cheng, *J. Mol. Struct. (Theochem)* 469 (1999) 127.
- [8] M. Yanagida, A. Takahara, T. Kajiyama, *Bull. Chem. Soc. Jpn.* 73 (2000) 1429.
- [9] M. Yanagida, T. Kuri, T. Kajiyama, *Chem. Lett.* 26 (1997) 911.
- [10] T. Imae, Y. Ikeo, *Supramol. Sci.* 5 (1998) 61.
- [11] L. Liang, Y. Fang, *Spectrochim. Acta A* 69 (2008) 113.
- [12] T. Nakamura, H. Tachibana, M. Yumura, M. Matsumoto, R. Azumi, M. Tanaka, Y. Kawabata, *Langmuir* 8 (1992) 4.
- [13] Y.S. Obeng, A.J. Bard, *J. Am. Chem. Soc.* 113 (1991) 6279.
- [14] R. Back, R.B. Lennox, *J. Phys. Chem.* 96 (1992) 8149.
- [15] L.O.S. Bulhões, S.Y. Obeng, A.J. Bard, *Chem. Mater.* 5 (1993) 110.
- [16] R. Castillo, S. Ramos, J. Ruiz-García, *J. Phys. Chem.* 100 (1996) 15235.
- [17] A.K. Evans, *J. Phys. Chem. B* 102 (1998) 7016.
- [18] D. Felder, M. Gutiérrez Nava, M. del Pilar Carreón, J. Eckert, M. Luccisana, C. Schall, P. Masson, J. Gallani, B. Heninrich, D. Guillon, J. Nierengarten, *Helv. Chim. Acta* 85 (2002) 288.
- [19] U. Jonas, F. Cardullo, P. Belik, F. Diederich, A. Gügel, E. Harth, A. Herrmann, L. Isaacs, K. Müllen, H. Ringsdorf, C. Thilgen, P. Uhlmann, A. Vasella, C.A.A. Waldraff, M. Walter, *Chem. Eur. J.* 1 (1995) 243 and references therein.
- [20] F. Cardullo, F. Diederich, F. Echegoyen, T. Habicher, N. Jayaraman, R.M. Leblanc, J.F. Stoddart, S. Wang, *Langmuir* 14 (1998) 1955.
- [21] K. Oh-ishi, J. Okamura, T. Ishi-i, M. Sano, S. Shinkai, *Langmuir* 15 (1999) 2224.
- [22] P. Wang, B. Chen, R.M. Metzger, T. Da Ros, M. Prato, *J. Mater. Chem.* 7 (1997) 2397.
- [23] J. Milliken, D.D. Dominguez, H.H. Nelson, W.R. Barger, *Chem. Mater.* 4 (1992) 252.
- [24] X. Li, S. Yang, Y. Xu, Y. Liu, D. Zhu, *Thin Solid Films* 413 (2002) 231.
- [25] Y. Gao, X.Z. Tang, E. Watkins, J. Majewski, H.L. Wang, *Langmuir* 21 (2005) 1416.

- [26] Y. Tian, J.H. Fendler, H. Hungerbühler, D.M. Guldi, K.-D. Asmus, *Mater. Sci. Eng. C* 7 (1999) 67.
- [27] S. Uemura, M. Sakata, C. Hirayama, M. Kunitake, *Langmuir* 20 (2004) 9198.
- [28] P. Moriarty, M.D.R. Taylor, M. Brust, *Phys. Rev. Lett.* 89 (2002) 248303.
- [29] C.P. Martin, M.O. Blunt, E. Pauliac-Vaujour, A. Stannard, P. Moriarty, I. Vancea, U. Thiele, *Phys. Rev. Lett.* 99 (2007) 116103.
- [30] E. Rabani, D.R. Reichman, P.L. Geissler, L.E. Brus, *Nature* 426 (2003) 271.
- [31] E. Pauliac-Vaujour, A. Stannard, C.P. Martin, M.O. Blunt, I. Notinger, P.J. Moriarty, I. Vancea, U. Thiele, *Phys. Rev. Lett.* 100 (2008) 176102.
- [32] Y.R. Ma, P. Moriarty, P.H. Beton, *Phys. Rev. Lett.* 78 (1997) 2588.
- [33] Hydrophobic silicon substrates were also prepared using a standard HF:NH<sub>4</sub>F treatment [Higashi, G.S. et al., *Appl. Phys. Lett.* **1990**, 56, 656]. However, neither C<sub>60</sub> nor C<sub>60</sub>O Langmuir films were transferred to hydrophobic silicon surfaces using a vertical dipping method. At best, a very small areal density of three dimensional clumps of molecules was observed. We did not attempt a horizontal transfer method for this study.